Discover Applied Sciences

Research

Comprehensive bioinformatics assessments of the ROP34 of *Toxoplasma gondii* to approach vaccine candidates

Fatemeh Mohammadhasani[1] · **Ali Dalir Ghaffari**[2] · **Masoumeh Asadi**[1]

Received: 12 July 2024 / Accepted: 5 September 2024
Published online: 18 September 2024

Abstract

Introduction Rhoptries proteins (ROPs) are crucial throughout different stages of the *Toxoplasma gondii* (*T. gondii*) lifecycle, playing key roles in both the invasion of host cells and their subsequent survival. ROP34 is particularly noteworthy as it significantly influences host gene expression and aids in the transition from the tachyzoite to the bradyzoite form.

Materials and methods This research utilized various bioinformatics tools to assess physico-chemical properties, allergenic and antigenic characteristics, sites for post-translational modifications (PTMs) and protein's secondary and three-dimensional structures of the ROP34 protein. Furthermore, the study identified potential B-cell, MHC-binding, and cytotoxic T-lymphocyte (CTL) epitopes within the ROP34 sequence.

Results The ROP34 peptide comprised 553 amino acid residues, with a calculated average molecular weight (MW) of 61.60149 kDa, an aliphatic index of 73.98, and a GRAVY score of − 0.554. The antigenicity of the multi-epitope peptide was estimated to be 0.526563 and 0.6025 by the ANTIGENpro and VaxiJen servers, respectively, suggesting ROP34 as an immunogenic protein with no allergenic potential. Secondary structure analysis revealed a composition of 52.80% random coil, 36.17% alpha helix, and 11.03% extended strand. The Ramachandran plot for the refined model depicted that 97.46% of the residues were situated in the favored region.

Conclusion This in silico research serves as a foundation for designing effective immunization tactics to target toxoplasmosis. The present article lays the groundwork for future studies and offers perspectives for the advancement of an appropriate toxoplasmosis vaccine.

Supplementary Information The online version contains supplementary material available at https://doi.org/10.1007/s42452-024-06189-2.

✉ Ali Dalir Ghaffari, a.dalirghafari@shahed.ac.ir; Fatemeh Mohammadhasani, fafatemeh.mh2004@gmail.com; Masoumeh Asadi, asadimsm.uiac@gmail.com | [1]Student Research Committee, Faculty of Medicine, Shahed University, Tehran, Iran. [2]Department of Parasitology and Mycology, Faculty of Medicine, Shahed University, Tehran, Iran.

Graphical Abstract

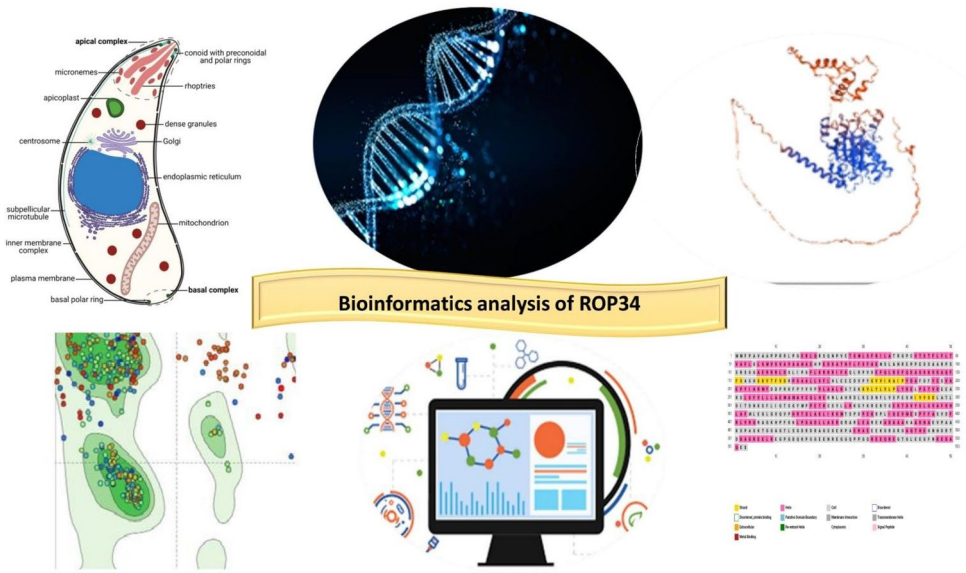

Highlights

- Toxoplasmosis represents a significant global concern, especially for pregnant individuals and those with weakened immune systems
- This article provided a comprehensive definition of the important aspects of the ROP34 protein using several bioinformatics tools.
- We present insightful bioinformatics insights regarding the ROP34 protein, demonstrating its potential as a future vaccine choice.

Keywords *Toxoplasma gondii* · ROP34 · Bioinformatics analysis · Vaccine

1 Introduction

Toxoplasma gondii (*T. gondii*) as an obligate intracellular parasite is classified under the phylum Apicomplexa. Cats serve as the main hosts for this parasite, while a variety of warm-blooded vertebrates such as marine mammals, humans, livestock, and birds act as intermediate hosts [1–3]. Surveys on the prevalence of *T. gondii* suggest that it is widely distributed and has a high occurrence rate in various regions worldwide [4, 5]. Human infection can happen through ingesting oocysts excreted by cats, consuming contaminated meat containing tissue cysts, or through congenital transmission [6–8]. In immunocompetent individuals, toxoplasmosis is typically asymptomatic; however, in immunocompromised patients, it can lead to severe and life-threatening complications [9]. In pregnant women, acute infections can lead to severe consequences in the fetus, including hydrocephalus, miscarriage, vision impairment, and cognitive disabilities [10]. *T. gondii* infections can trigger encephalitis by reactivating dormant cysts in individuals with weakened immune systems [11], making it a significant opportunistic pathogen in HIV patients [12]. Among livestock, toxoplasmosis can cause abortions, stillbirths, and deaths in newborn animals, resulting in considerable economic losses. Infected livestock serve as a primary infection source for humans [13]. Presently, there is no perfect medication available for preventing or treating *T. gondii* infections. Nonetheless, existing insights into protective immunity against *T. gondii* infections propose that vaccination could serve as a feasible approach for disease management [14]. Bioinformatics stands out as a contemporary research domain employed to tackle biological challenges more efficiently [15]. This field is widely applied for gene and protein expression analysis, protein structure prediction, assessment of immunogenicity, and overall characteristics. Through the examination of physical, chemical, and

immunogenic attributes of proteins, researchers can deepen their comprehension of these molecules and pinpoint suitable epitopes for vaccine development [16]. Using bioinformatics strategies for identifying protein epitopes is invaluable for diagnostic applications and vaccine production [17]. Improving computational approaches increases the reliability of in silico methods in biological studies [18]. Depending on this, the methods are often preferred for predicting antigenic proteins even if they are not expressed in vitro [18]. In silico methods also offer several advantages such as time/effort and cost-effectiveness. For this reason, in silico methods are essential as a pre-analysis strategy prior to starting wet lab investigations [18]. Although the number of proteins can be easily predicted using in silico methods for antigen discovery, a very important step in vaccine design studies, as a further recommendation, three conditions should be considered; Choosing the right analysis tools, using multiple parameters to get the right results, and further validating them through wet lab studies [18]. It is important to recognize that the continuous efforts of scientists in developing candidate vaccines for *T. gondii* have yielded significant advancements with key antigens, like surface antigens (SAG), microneme antigens (MIC), dense granule antigens (GRA), and ROP antigens [19]. Among these, ROPs are particularly noteworthy as promising vaccine candidates because of their distinctive performance [20]. Proteins encoded by the ROP family genes are promising candidates for DNA vaccines, with several members such as ROP5, ROP18, ROP17, and ROP19 being identified as promising vaccine candidates against *T. gondii* [21–24]. Similar to other ROP proteins, ROP34 is localized to the rhoptries. However, its structure and epitopes remain not well-defined. Hence, the current study aimed to precisely assess the bioinformatics characteristics of the ROP34 protein from *T. gondii*. This involved examining various aspects such as allergenicity, antigenicity, physico-chemical properties, signal peptide, post-translational modification (PTM) sites, transmembrane domains, structural analysis, and subcellular localization. Additionally, comprehensive immunoinformatics approaches were employed to predict the epitopes of helper T-lymphocyte (HTL) and cytotoxic T-lymphocyte (CTL) associated with these proteins.

2 Material and methods

2.1 Amino acid sequence

Initially, the complete ROP34 amino acid sequence was achieved from the National Center for Biotechnology Information (NCBI), a publicly accessible sequence database. Links to all bioinformatics web servers used in this study are provided in Supplementary Table 1.

2.2 Predicting physico-chemical properties

To determine the physico-chemical properties of ROP34, the Expasy ProtParam tool was used. This analysis provided information on amino acid composition, protein molecular weight (MW), aliphatic index (AI), grand average of hydropathicity (GRAVY), isoelectric point (pI), instability index (II), extinction coefficients, in vivo and in vitro half-life, as well as the residue numbers with negative and positive charges [25].

2.3 Allergenicity, antigenicity, and solubility assessment

The ANTIGENpro [26] and VaxiJen 2.0 [27] servers assessed the ROP34 protein antigenicity. ANTIGENpro predicts antigenicity based solely on microarray data, with no relying on pathogen and alignment data. In contrast, VaxiJen uses a novel alignment-free approach, transforming sequences through auto cross covariance (ACC) into vectors of principal amino acid properties. The accuracy of VaxiJen predictions ranges between 70 and 89% depending on the target organism (http://www.ddg-pharmfac.net/vaxijen/VaxiJen/VaxiJen_help.html). Additionally, allergenicity was predicted using the AlgPred server, which employs a hybrid approach (IgE epitope + SVMc, ARPs Blast + MAST) with 85% accuracy and a threshold of – 0.4 [28]. The SOLpro server predicted the solubility of the protein after overexpression [29].

2.4 Signal peptide prediction and post-translational modification (PTM) sites of ROP34

The SignalP server identified the presence of signal peptides in the sequence. The protein had a Sec signal peptide (Sec/SPI), a Lipoprotein signal peptide (Sec/SPII), a Tat signal peptide (Tat/SPI), or no signal peptide at all (Other) [30]. Phosphorylation sites for tyrosine, threonine, and serine, were identified using neural network ensembles in the NetPhos 3.1 server [31]. Additionally, GPS-PAIL 2.0 [32] was used to detect possible acylation sites in the ROP34 sequence. Furthermore, the

NetNGlyc1.0 [33] and NetOGlyc 4.0 servers respectively anticipated N-linked glycosylation and O-linked glycosylation regions [34]. The NetNGlyc1.0 server determined N-linked glycosylation sites by selecting "Predict on all Asn residues," and default features were applied for the O-linked glycosylation areas.

2.5 Identification of subcellular localization and transmembrane domains

The PSORT II server predicted the ROP34 subcellular localization. Additionally, the protein transmembrane domains were assessed by the TMHMM 2.0 server [35].

2.6 Prediction of tertiary and secondary structures

The Garnier-Osguthorpe-Robson (GOR) server predicted the secondary structure [36]. To further elucidate the ROP34 secondary structure, the PSIPRED server was utilized for position-specific iterated anticipation, by the outputs of PSI-BLAST [37]. Disulfide bonds within the protein were predicted by the DIpro server [38]. The ROP34 sequence 3D models were generated through homology modeling using the SWISS-MODEL server [35–39].

2.7 Tertiary structure confirmation and refinement

Of the developed templates and built models using SWISS-MODEL, one characterized by suitable sequence identity and coverage was considered for refinement using the GalaxyRefine online server, working following the CASP10-tested method [40, 41]. It can rearrange side chains, repack them, and relax the entire structure through molecular dynamics simulation. The SWISS-MODEL server generated Ramachandran plots for validating the tertiary structure [42]. According to Narula et al., the "Ramachandran plot is utilized to predict the likelihood of a particular amino acid forming secondary structures based on the dihedral angles ϕ and Ψ (allowed and disallowed) of amino acids, which are calculated based on the van der Waals radius of side chain atoms" [43].

2.8 Predicting conformational and linear B-cell epitopes

Several servers predicted linear B-cell epitopes. Initially, the ABCpred server identified the linear B-cell epitopes [44]. Additionally, these epitopes were predicted using the Bcepred web-based algorithm. Continuous B-cell epitopes were predicted by the Bcepred tool, with 58.7% accuracy considering physico-chemical characteristics, like antigenic propensity, hydrophilicity, exposed surface, accessibility, polarity, flexibility, and turns [45, 46]. Furthermore, the B-cell epitopes were predicted by BCPREDS 1.0 with the default specificity of 75% and 20-mer epitopes [47] and SVMTriP [48]. The ProtScale tool generated a graphical representation of linear epitopes, using hydrophobicity, mean flexibility, alpha-helix, beta-turn, and the percentage of accessible residues [25]. The ElliPro server anticipated discontinuous B-cell epitopes. Each epitope receives a protrusion index (PI), which is the average of its residues. ElliPro uses ellipsoids for these calculations; for example, a PI value of 0.8 indicates that 80% of residues are within the ellipsoid, while the rest are outside. Residues with higher PI values are linked to greater solvent accessibility. Additionally, the R distance, which is the interval between a residue's mass center measured in Angstroms, affects the clustering of epitopes. An increase in the R value suggests a higher number of conformational B-cell epitopes [49]. These immune epitope database (IEDB) further identified epitopes. Finally, the VaxiJen 2.0, AllergenFP 1.0 [50], and PepCalc servers evaluated antigenicity, allergenicity, and water solubility of the epitopes, respectively.

2.9 Predicting major histocompatibility complex (MHC)-specific epitopes

The Immune Epitope Database (IEDB) recommended method was utilized to predict the half-maximal inhibitory concentration (IC_{50}) scores of peptides binding to MHC class I and II molecules. Specifically, predictions were made for MHC-I specific epitopes (10-mers) for mouse alleles H2-Db, H2-Dd, H2-Kb, H2-Kd, H2-Kk, and H2-Ld. Additionally, predictions were conducted for MHC-II epitopes (15-mers) for mouse alleles H2-IAb, H2-IAd, and H2-IEd. Furthermore, forecasts were conducted with peptides consisting of ten amino acids employing the IEDB recommended technique. Subsequently, the identified epitopes underwent immunogenicity prediction utilizing the IEDB MHC Class I immunogenicity prediction tool [51]. The prediction process adhered to the IEDB recommended methodology, with the expected peptide length set

at 15 amino acids and arranged by percentile rank. Following this, the antigenicity and the potential for IFN-γ and IL-4 induction for each epitope were forecasted using the VaxiJen v2.0, IFNepitope, and IL4-pred online platforms, respectively.

2.10 Prediction of cytotoxic T lymphocyte (CTL) epitopes

Finally, CTL epitopes were analyzed and predicted by the CTLpred tool was following a combined method with 75.8% accuracy. The cutoff points for the support vector machine (SVM) and artificial neural network (ANN) were respectively set at 0.51 and 0.36 [52]. Subsequently, the IEDB MHC Class I immunogenicity prediction tool anticipated the immunogenicity of the epitopes [51].

2.11 Immune simulation

The C-ImmSim server predicted the virtual immunological simulation process that was provoked by ROP34 [53]. As previously shown, the minimum time between each injection is a four-week interval and is usually recommended for a standard clinical protocol [54]. Thus, the server was set for three inoculation doses of ROP34 at four-week intervals with time points of 1, 84, and 168 (each time point is equivalent to eight h). Other settings for this computer-aided simulation included a simulation volume of 50, 1050 simulation steps, and a random seed of 12,345.

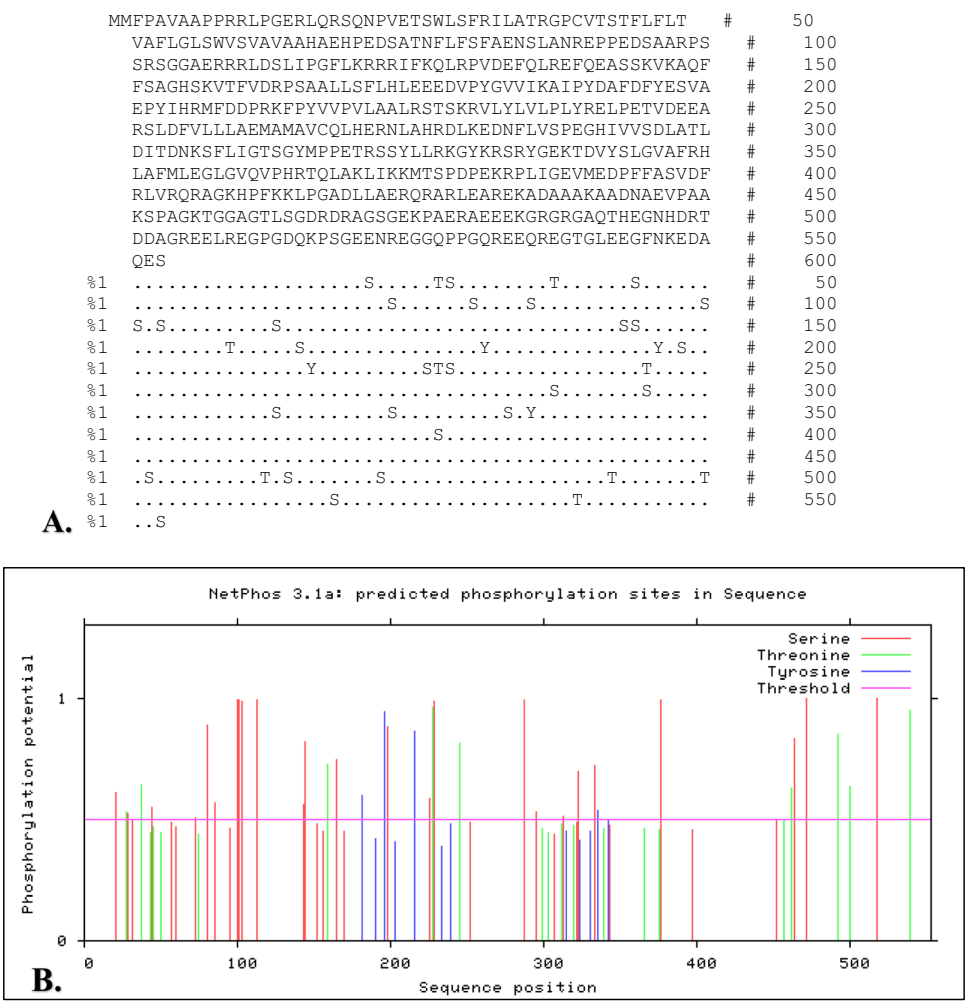

Fig. 1 NetPhos server output for ROP34 phosphorylation sites. **A** The number of predicted sites, based on S (serine), T (threonine) and Y (tyrosine); **B** Prediction diagram of ROP34 phosphorylation sites (http://www.cbs.dtu.dk/services/NetPhos-2.0/output.php)

Table 1 Acetylation sites predicted using GPS-PAIL 2.0 server with Medium threshold

ID	Position	Peptide	Score	Cutoff
1	409	LVRQRAGKHPFKKLP	2.855	1.382
2	414	AGKHPFKKLPGADLL	1.349	1.343
3	440	EKADAAAKAADNAEV	0.46	0.42
4	451	NAEVPAAKSPAGKTG	0.476	0.42
5	456	AAKSPAGKTGGAGTL	1.449	1.382
6	475	DRAGSGEKPAERAEE	1.667	1.382
7	484	AERAEEEKGRGRGAQ	1.507	1.382
8	516	REGPGDQKPSGEENR	1.496	1.348
9	547	GLEEGFNKEDAQES*	1.952	1.348

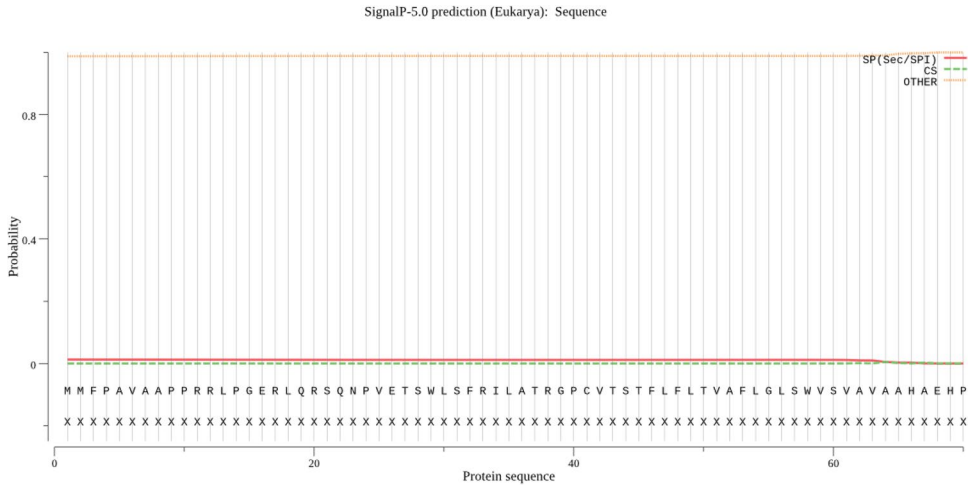

Fig. 2 Signal peptide prediction of the ROP34 protein of *T. gondii*, using SignalP-5.0 online tool. SP (Sec/SPI): type of signal peptide predicted; CS: the cleavage site; Other: the probability that the sequence does not have any kind of signal peptide

3 Results

3.1 General features of *T. gondii* ROP34 gene

The NCBI database retrieved the amino acid sequence of the *T. gondii* ROP34 gene in FASTA format. It comprises 553 amino acid residues with a theoretical pI of 6.29 and a MW of 61,601.49 Da. The sequence contains 79 positively charged residues (Lys + Arg) and 84 negatively charged residues (Glu + Asp). It has 8638 atoms and an extinction coefficient of 29,005 M^{-1} cm^{-1} in water at 280 nm. The ROP34 protein estimated half-life is over 20 h in yeast (in vivo), 30 h in mammalian reticulocytes (in vitro), and over 10 h in *Escherichia coli* (*E. coli*) (in vivo). The II score is 49.66, classifying the protein as unstable. Additionally, the AI and GRAVY were respectively 73.98 and − 0.554.

3.2 Allergenicity, antigenic properties, and solubility evaluation

The ROP34 antigenicity was 0.526563 by ANTIGENpro and 0.6025 by VaxiJen, with a threshold of 0.5. The AlgPred hybrid method evaluated the allergenicity of ROP34, which indicated that ROP34 is a non-allergen. Furthermore, the SOLpro server predicted that the protein, when overexpressed in *E. coli*, would be soluble with a likelihood of 0.598.

3.3 Prediction of PTM sites of ROP34

According to the NetPhos 3.1 analysis, the ROP34 protein sequence contains 40 phosphorylation sites, including 27 serine, 9 threonine, and 4 tyrosine residues (Fig. 1). Additionally, the protein has 9 acetylation sites as determined using a medium threshold setting (Table 1). The SignalP Server predicted a Sec signal peptide (Sec/SPI) in the ROP34

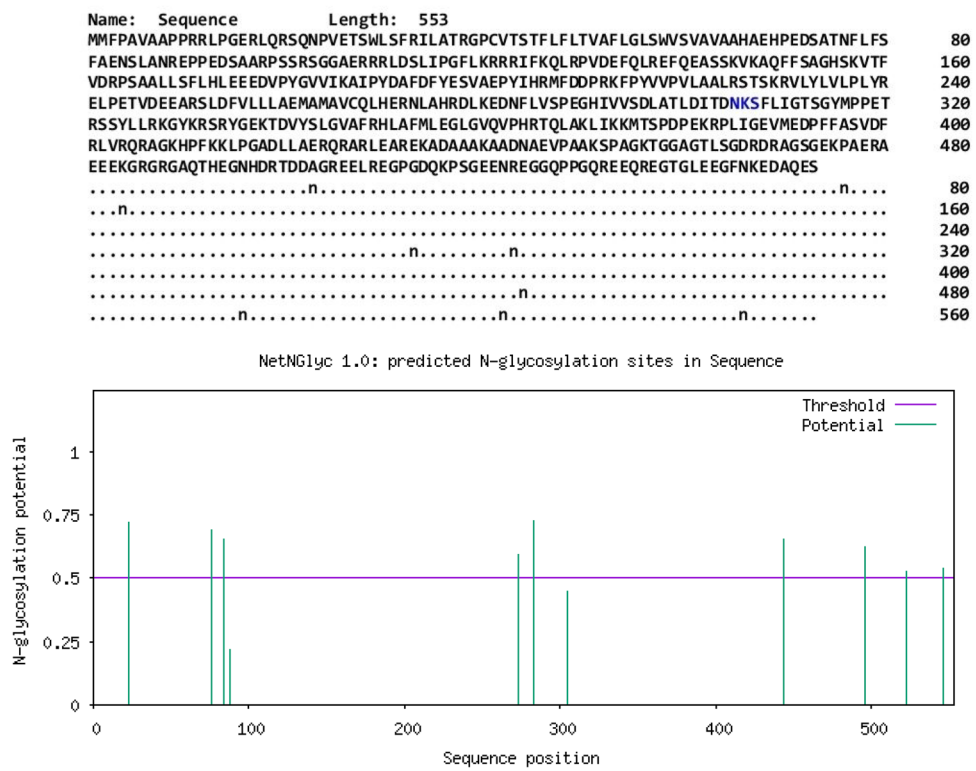

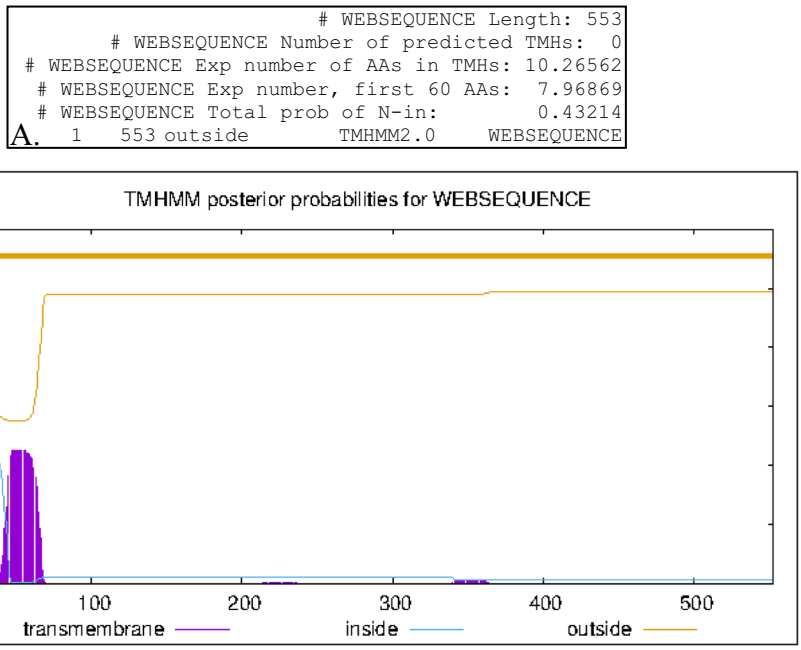

Fig. 3 The output from NetNGlyc server for N-glycosylation sites of ROP34

Fig. 4 Bioinformatics analysis of transmembrane domain of ROP34 sequence. **A** Number of predicted TMHs: The number of predicted transmembrane helices; Exp number of AAs in TMHs: The expected number of amino acids in transmembrane helices. If this number is larger than 18 it is very likely to be a transmembrane protein (OR have a signal peptide); Exp number, first 60 AAs: The expected number of amino acids in transmembrane helices in the first 60 amino acids of the protein. If this number more than a few, you should be warned that a predicted transmembrane helix in the N-term could be a signal peptide; Total prob. of N-in: The total probability that the N-term is on the cytoplasmic side of the membrane; POSSIBLE N-term signal sequence: a warning that is produced when "Exp number, first 60 AAs" is larger than 10 (https://services.healthtech.dtu.dk/services/TMHMM-2.0/); **B** Graphical illustration of transmembrane domain analysis of ROP34

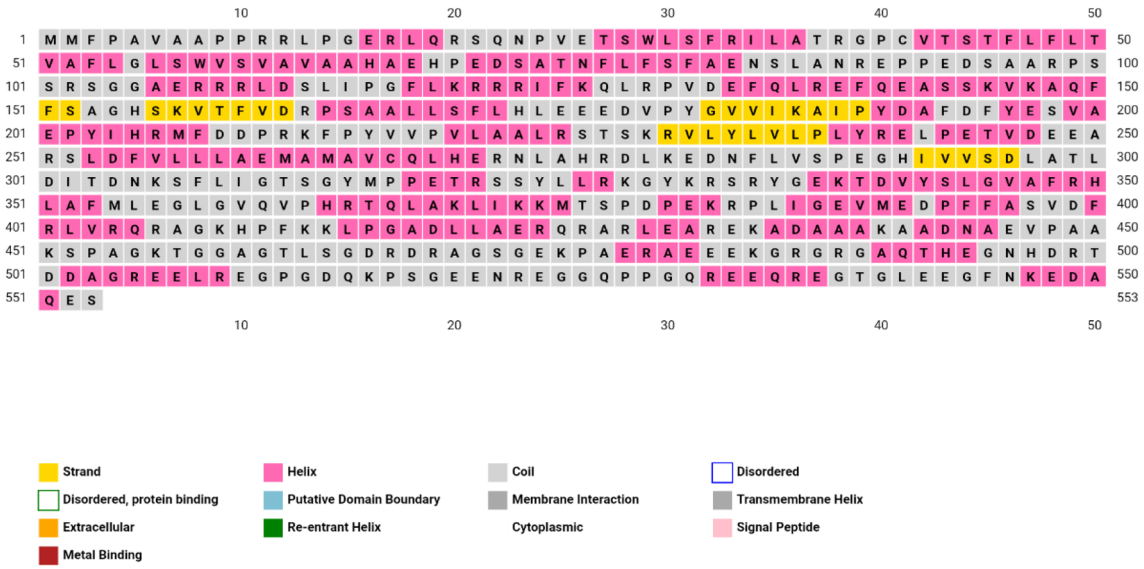

Fig. 5 Analysis of secondary structure of ROP34 using GOR IV. **A** Predicted secondary structure. **B** Graphical frame of secondary structure prediction of ROP34 protein. h, helix; e, extended strand; c, coil

Fig. 6 Graphical result from secondary structure prediction of vaccine using PSIPRED

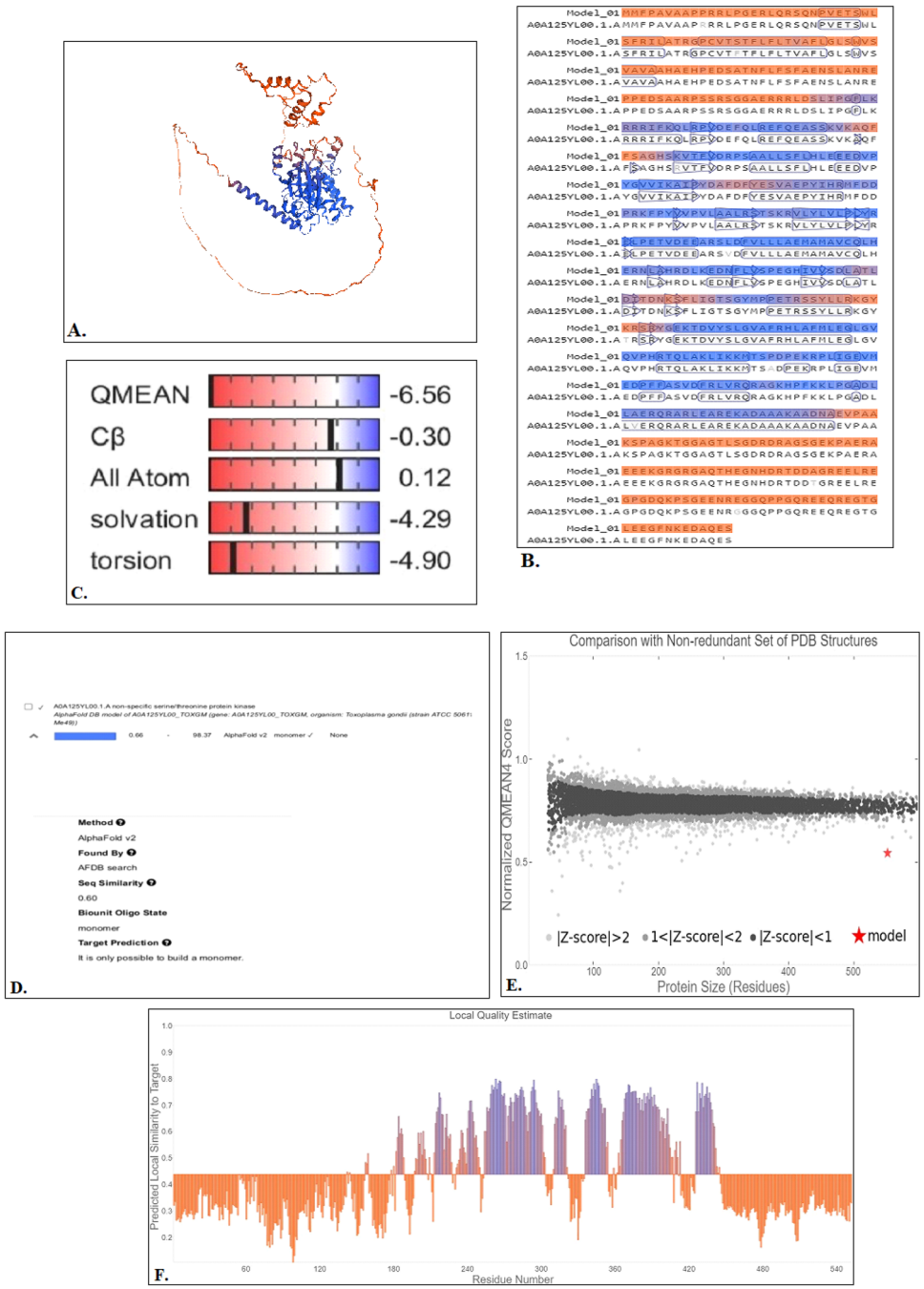

Fig. 7 SWISS-MODEL server output of ROP38. **A** Computed 3D model; **B** Model-template alignment; **C** Global quality estimate; **D** Sequence identity and coverage; **E** Comparison with non-redundant set of PDB structures; and **F** Local quality estimate

protein with a possibility of 0.9878 (Fig. 2). Furthermore, the ROP34 protein had 9 N-linked glycosylation sites (Fig. 3) and 19 O-linked glycosylation areas.

3.4 Prediction of subcellular localization and transmembrane domains of ROP34

The subcellular localization assessment using PSORT II provided the following distribution: endoplasmic reticulum (44.4%), mitochondrial (22.2%), plasma membrane (11.1%), nuclear (11.1%), and golgi apparatus (11.1%). Additionally, the TMHMM server analysis indicated that the ROP34 sequence does not contain any transmembrane domains (Fig. 4).

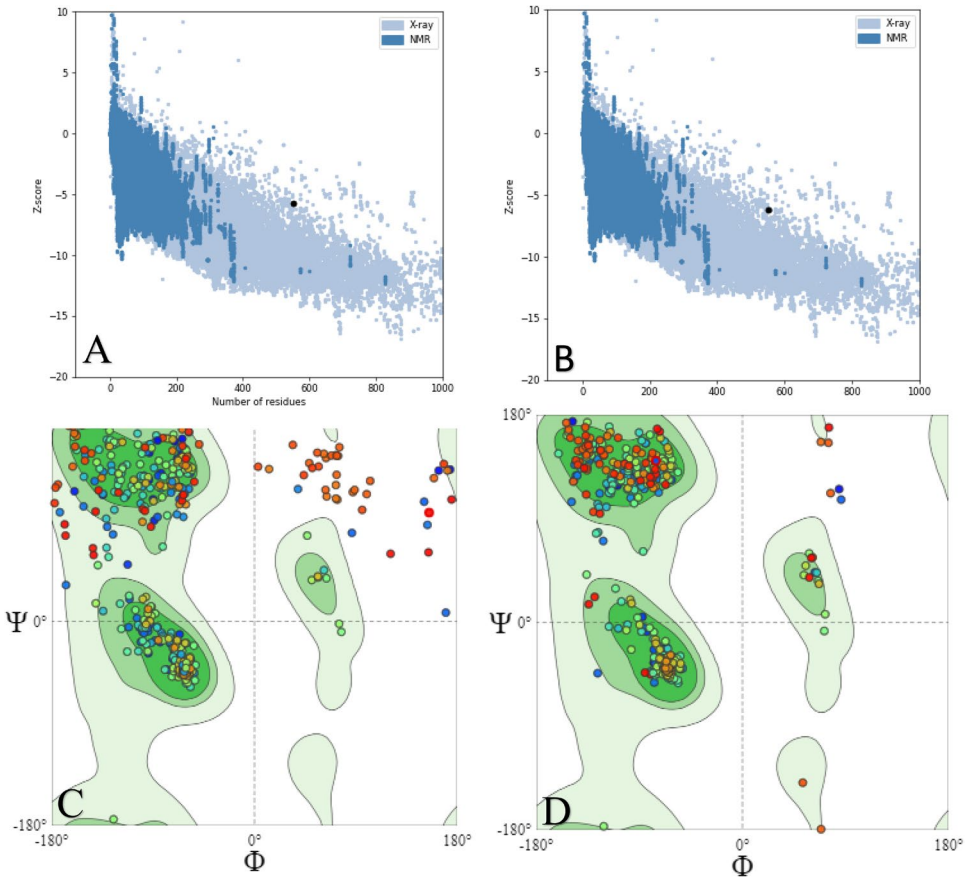

Fig. 8 Validation of the 3D structure of ROP34 protein using Ramachandran plot. **A** The Z-score plot for 3D structure of predicted vaccine before refinement was assessed to be -5.76. **B** The Z-score plot for 3D structure of predicted vaccine after refinement was assessed to be -6.23. The analysis of Ramachandran plot using SWISS-MODEL server in initial model (**C**), the model after refinement (**D**)

Table 2 Predicted B-cell epitope using ABCpred server

Rank	Sequence	Start position	Score	Vaxijen score	Allergenicity	Water solubility
1	THEGNHDRTDDAGREE	492	0.94	1.1613	ALLERGEN	Good
2	AERQRARLEAREKADA	422	0.93	1.0588	ALLERGEN	Good
2	AKLIKKMTSPDPEKRP	369	0.93	0.1107	ALLERGEN	Good
3	KGRGRGAQTHEGNHDR	484	0.90	1.8559	NON-ALLERGEN	Good
4	RPSSRSGGAERRRLDS	98	0.89	0.4623	ALLERGEN	Good
4	YESVAEPYIHRMFDDP	196	0.89	0.0085	ALLERGEN	Good
5	TSGYMPPETRSSYLLR	312	0.87	0.5970	NON-ALLERGEN	Good
6	SFRILATRGPCVTSTF	31	0.86	0.1710	NON-ALLERGEN	Poor
6	HIVVSDLATLDITDNK	291	0.86	−0.1803	ALLERGEN	Good
7	AGREELREGPGDQKPS	503	0.85	0.4960	NON-ALLERGEN	Good
7	SRYGEKTDVYSLGVAF	333	0.85	0.8432	ALLERGEN	Good
8	AFMLEGLGVQVPHRTQ	352	0.84	0.8314	ALLERGEN	Poor
8	HRMFDDPRKFPYVVPV	205	0.84	0.3903	ALLERGEN	Good
9	YRELPETVDEEARSLD	239	0.83	0.1105	ALLERGEN	Good
10	EQREGTGLEEGFNKED	534	0.82	0.3364	ALLERGEN	Good
10	YLLRKGYKRSRYGEKT	324	0.82	1.2090	ALLERGEN	Good
10	AIPYDAFDFYESVAEP	187	0.82	−0.1036	ALLERGEN	Good
11	QRAGKHPFKKLPGADL	405	0.82	−0.1098	ALLERGEN	Good
11	IGEVMEDPFFASVDFR	386	0.81	1.2150	ALLERGEN	Good
12	PEDSAARPSSRSGGAE	92	0.81	0.9870	NON-ALLERGEN	Good
12	GDQKPSGEENREGGQP	513	0.80	1.6042	ALLERGEN	Good
12	GTLSGDRDRAGSGEKP	461	0.80	1.6406	NON-ALLERGEN	Good
12	GKTGGAGTLSGDRDRA	455	0.80	1.7482	NON-ALLERGEN	Good

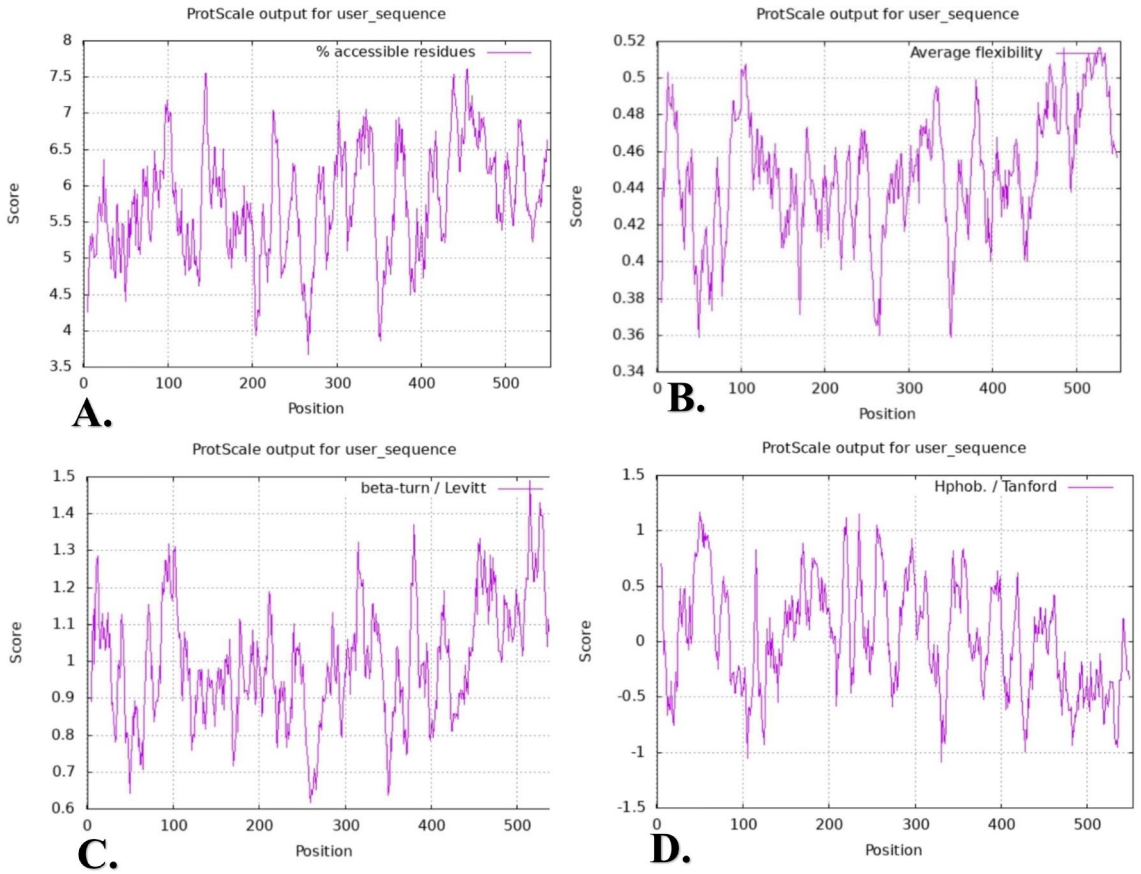

Fig. 9 Linear B-cell epitopes of ROP34 protein sequence based on **A** percent of accessible residues, **B** average flexibility, **C** beta turn and **D** hydrophobicity

Table 3 The predicted B-cell epitopes, using physico-chemical properties based on Bcepred server

Prediction parameter	Epitope sequence
Hydrophilicity	HAEHPEDSATN,ANREPPEDSAARPSSRSGGAERRR,PETVDEEARS,RDLKEDN,DITDNKS,PPETRSS,KRSRYGEKTD,TSPDPEKRP,EAREKADAAAKAADNAE,KSPAGKTGGAGTLSGDRDRAGSGEKPAERAEEEKGRGRGAQTHEGNHDRTDDAGREE,REGPGDQKPSGEENREGGQPPGQREEQREGTG,EEGFNKEDAQES
Flexibility	LPGERLQRSQ,SLANREP,DSAARPSSRSGGAERRRL,REFQEASSKV,LAALRSTSK,ETVDEEA,GYMPPETR,YLLRKGYKRSRYG,KMTSPDPEK,RLVRQRA,LLAERQR,PAAKSPA,GTLSGDRDRAGSGE,PAERAEEEKGRGRG,EELREGPGDQKPSGEENREGGQPPGQREEQREG
Accessibility	AAPPRRLPGERLQRSQNPVETS,HAEHPEDSATN,ENSLANREPPEDSAARPSSRSGGAERRRLDSL,PGFLKRRRIFKQLRPVDEFQLREFQEASSKVKAQ,LEEEDVPYG,AEPYIHRMFDDPRKFPYV,ALRSTSKRVLY,PLYRELPETVDEEARSLD,QLHERNLAHRDLKEDNF,LDITDNKS,YMPPETRSSYLLRKGYKRSRYGEKTDVYS,QVPHRTQLAKLIKKMTSPDPEKRPLI,FRLVRQRAGKHPFKKLPGADLLAERQRARLEAREKADAA,KAADNAE,AKSPAGKT,LSGDRDRAGSGEKPAERAEEEKGRGRGAQTHEGNHDRTDDAGREELREGPGDQKPSGEENREGGQPPGQREEQREGTG,EEGFNKEDAQES
Turns	HEGNHDRT
Exposed Surface	ERLQRSQN,NREPPEDS,AERRRLDS,KRRRIFKQ,DDPRKFPY,HRDLKEDN,LRKGYKRSRYGEKTD,KLIKKMTSPDPEKRPL,GKHPFKKL,AERQRARLEAREKAD,EKPAERAEEEKGRGR,QKPSGEE,PGQREEQREG,NKEDAQES
Polarity	PRRLPGERLQRSQ,VAAHAEHPEDSA,ANREPPEDS,RSGGAERRRLDSL,PGFLKRRRIFKQLR,DEFQLREFQEASSKVK,SFLHLEEEDVPY,AEPYIHRMFDDPRKFP,LRSTSKRV,LYRELPETVDEEARSLD,VCQLHERNLAHRDLKEDNF,LLRKGYKRSRYGEKTD,HRTQLAK,SPDPEKRPLIGE,FRLVRQRAGKHPFKKLP,LLAERQRARLEAREKADAA,LSGDRDRAGSGEKPAERAEEEKGRGRGAQTHEGNHDRTDDAGREELREGPG,QKPSGEENREGGQPPGQREEQREGTGLEEGFNKEDAQES
Antigenic Propensity	PCVTSTFLFLTV,FLGLSWVSV,SLIPGFLK,FKQLRPV,HSKVTFV,LLSFLHLE,DVPYGVVIK,RKFPYVVPVLA,SKRVLYLVLPLYREL,RSLDFVLLL,VCQLHER,PEGHIVVSDL,DVYSLGV,EGLGVQVPHRT,SVDFRLVR

Table 4 BCPreds predictions of linear B-cell epitopes from ROP34 protein

No	Position	Epitope	Score	Vaxijen score	Allergenicity	Water solubility
1	520	EENREGGQPPGQREEQREGT	1	1.5468	ALLERGEN	Good
2	442	ADNAEVPAAKSPAGKTGGAG	1	1.2008	NON-ALLERGEN	Good
3	469	RAGSGEKPAERAEEEKGRGR	1	1.1669	NON-ALLERGEN	Good
4	86	LANREPPEDSAARPSSRSGG	1	0.7107	NON-ALLERGEN	Good
5	7	AAPPRRLPGERLQRSQNPVE	0.999	0.6371	ALLERGEN	Good
6	499	RTDDAGREELREGPGDQKPS	0.997	0.6285	NON-ALLERGEN	Good
7	174	LEEEDVPYGVVIKAIPYDAF	0.998	0.4106	Potential ALLERGEN	Good
8	197	ESVAEPYIHRMFDDPRKFPY	0.956	−0.0262	ALLERGEN	Good
9	369	AKLIKKMTSPDPEKRPLIGE	0.951	0.3654	NON-ALLERGEN	Good
10	305	NKSFLIGTSGYMPPETRSSY	0.951	0.7251	NON-ALLERGEN	Poor
11	399	DFRLVRQRAGKHPFKKLPGA	0.917	−0.1134	NON-ALLERGEN	Good
12	65	AHAEHPEDSATNFLFSFAEN	0.828	0.4903	ALLERGEN	Good
13	234	LVLPLYRELPETVDEEARSL	0.781	0.6598	ALLERGEN	Good

Table 5 B-cell linear epitopes predicted using SVMTriP server

Rank	Location	Epitope	Score	Vaxijen score
1	150–169	FFSAGHSKVTFVDRPSAALL	1.000	0.0005
2	395–414	FASVDFRLVRQRAGKHPFKK	0.833	−0.0192
3	417–436	GADLLAERQRARLEAREKAD	0.596	0.6615
4	51–70	VAFLGLSWVSVAVAAHAEHP	0.560	0.6713
5	358–377	LGVQVPHRTQLAKLIKKMTS	0.493	0.5134
6	215–234	PYVVPVLAALRSTSKRVLYL	0.462	0.3531
7	119–138	LKRRRIFKQLRPVDEFQLRE	0.426	0.0484
8	492–511	THEGNHDRTDDAGREELREG	0.423	1.0741

3.5 Tertiary and secondary structure assessment

The GOR IV and PSIPRED servers predicted the secondary structure elements of the ROP34 protein sequence, including random coil, alpha helix, and extended strand (Figs. 5 and 6). According to the GOR IV analysis, the ROP34 protein consists of 292 (52.80%) random coil, 61 (11.03%) extended strand, and 200 (36.17%) alpha helix elements. Additionally, the analysis identified 23 cysteine residues in the ROP34 protein, which are expected to form disulfide bonds at specific positions, including residues 41 and 267. The ROP34 3D model was produced by the SWISS-MODEL tool. From the proposed models, the one with 98.37% sequence identity and high coverage was selected. Figure 7 shows the complete details of the SWISS-MODEL output.

3.6 Validation and refinement of the tertiary structure

The refinement process utilized the GalaxyRefine tool, determining that model 1 emerged as the most effectively refined template according to multiple parameters: RMSD (0.549), GDT-HA (0.9222), MolProbity (1.498), Poor rotamers (0.2), Clash score (7.1), and Rama favored (97.5). The ProSA-web online tool assessed model quality, which reported a Z-score of − 5.76 for the crude model and − 6.23 for the refined model (Fig. 8).

3.7 Conformational and linear B cell epitopes

The ABCpred server anticipated the linear B-cell epitopes with a 16-mer length, where higher scores indicate greater prediction reliability (Table 2). Additionally, B-cell specific epitopes were identified considering various physicochemical factors by the ProtScale and Bcepred servers (Fig. 9 and Table 3). Also, Tables 4 and 5 present the BCPREDs

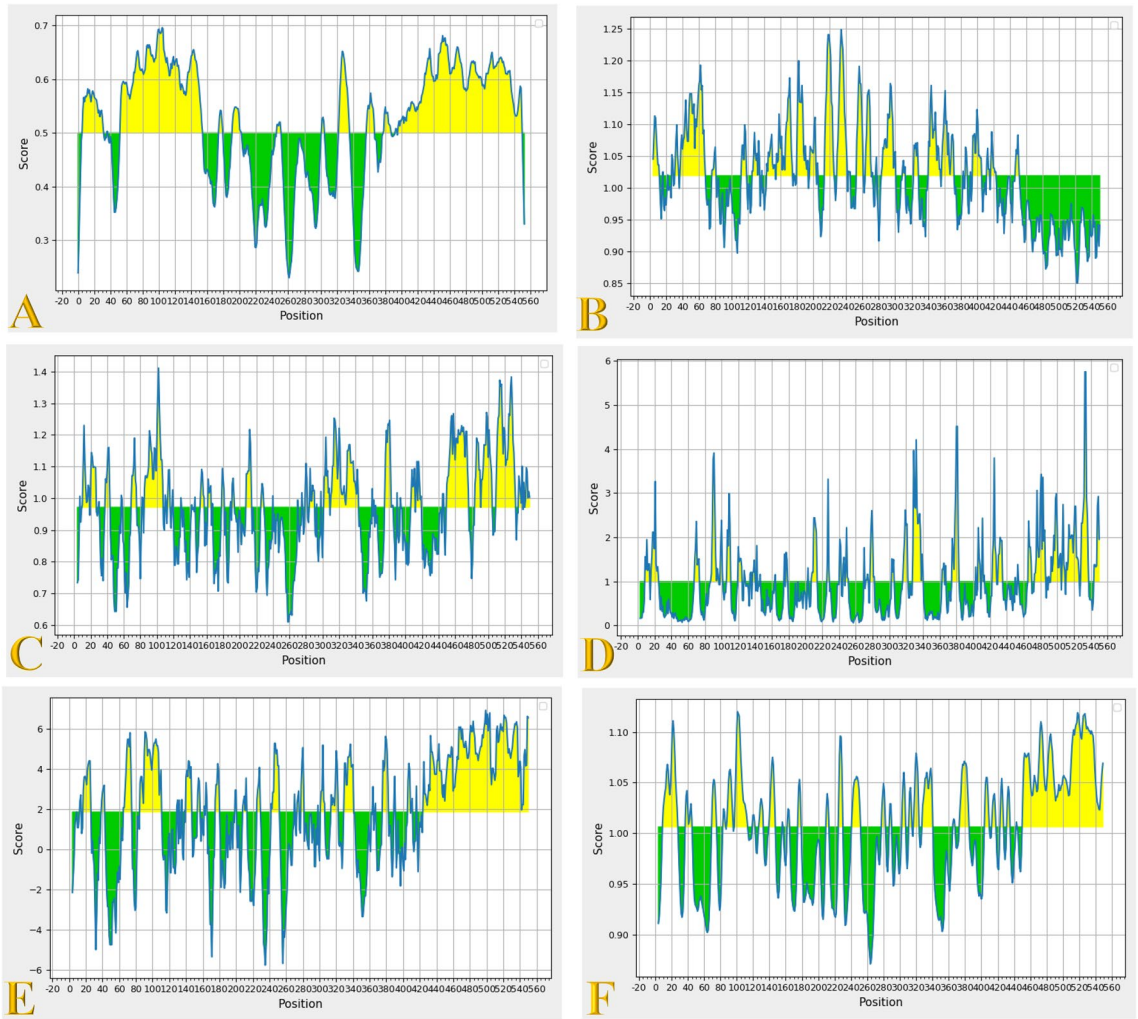

Fig. 10 Propensity scale plots of ROP34 protein. **A** Bepipred linear epitope prediction. **B** Antigenicity. **C** Beta-turn. **D** Surface accessibility. **E** Hydrophilicity. **F** Flexibility. On the graphs, the Y-axes depicts for each residue the correspondent score (averaged in the specified window), while the X-axes depicts the residue positions in the sequence. The tables provide values of calculated scores for each residue. The larger score for the residues might be interpreted as that the residue might have a higher probability to be part of epitope (those residues are colored in yellow on the graphs). Green color (below the threshold) indicate the unfavorable regions related to the properties of interest

and SVMTriP results. The average scores for beta-turn, antigenicity, hydrophilicity, Bepipred linear epitope prediction, surface accessibility and flexibility of the ROP34 protein, as determined by the IEDB online tool, were respectively 1.019, 1.866, 0.971, 0.522, 1.000, and 1.006 (Fig. 10). B-cell epitopes possessing proper solubility in water with appropriate antigenicity and negative allergenicity with ABCpred, BCPREDs, and SVMTriP were the followings, respectively: KGRGRGAQTHEGNHDR (VaxiJen score: 1.8559), ADNAEVPAAKSPAGKTGGAG (VaxiJen score: 1.2008), and GADLLAERQRARLEAREKAD (VaxiJen score: 0.6615). When predicting conformational B cell epitopes via ElliPro, sixteen discontinuous B cell epitopes were identified: 4 residues (score: 0.909), 27 residues (score: 0.89), 8 residues (score: 0.874), 8 residues (score: 0.881), 47 residues (score: 0.827), 6 residues (score: 0.759), 9 residues (score: 0.778), 5 residues (score: 0.752), 16 residues (score: 0.732), 5 residues (score: 0.689), 31 residues (score: 0.696), 19 residues (score: 0.682), 5 residues (score: 0.522), 45 residues (score: 0.576), 6 residues (score: 0.502), and 4 residues (score: 0.501) (Table 6 and Figs. 10, 11).

3.8 Predicting MHC-specific epitopes

Tables 7 and 8 comprehensively list the anticipated MHC-II (15-mer) and MHC-I (10-mer) epitopes, considering the estimated IC_{50} values for peptide binding to mouse-specific alleles. Related immunogenicity, antigenicity, IL-4 and IFN-γ

Table 6 Predicted discontinuous B-cell epitope residues of the ROP34 sequence

No	Residues	Number of residues	Score
1	A:L13, A:P14, A:G15, A:E16	4	0.909
2	A:G489, A:A490, A:Q491, A:T492, A:H493, A:E494, A:G495, A:N496, A:H497, A:D498, A:R499, A:T500, A:D501, A:D502, A:A503, A:G504, A:R505, A:E506, A:E507, A:L508, A:R509, A:E510, A:G511, A:P512, A:G513, A:D514, A:Q515	27	0.89
3	A:F3, A:P4, A:A5, A:V6, A:A7, A:A8, A:P9, A:P10	8	0.881
4	A:K516, A:P517, A:S518, A:G519, A:E520, A:E521, A:N522, A:R523	8	0.874
5	A:A438, A:A441, A:A442, A:D443, A:N444, A:A445, A:E446, A:V447, A:P448, A:A449, A:A450, A:K451, A:S452, A:P453, A:A454, A:G455, A:K456, A:T457, A:G458, A:G459, A:A460, A:G461, A:T462, A:L463, A:S464, A:G465, A:D466, A:R467, A:D468, A:R469, A:A470, A:G471, A:S472, A:G473, A:E474, A:K475, A:P476, A:A477, A:E478, A:R479, A:A480, A:E481, A:E482, A:E483, A:K484, A:G485, A:R486	47	0.827
6	A:E524, A:G525, A:G526, A:Q527, A:P528, A:P529, A:G530, A:Q531, A:R532	9	0.778
7	A:E548, A:D549, A:A550, A:Q551, A:E552, A:S553	6	0.759
8	A:N84, A:S85, A:L86, A:A87, A:N88	5	0.752
9	A:E90, A:P91, A:P92, A:E93, A:D94, A:S95, A:A96, A:A97, A:R98, A:P99, A:S100, A:S101, A:S103, A:G104, A:G105, A:A106	16	0.732
10	A:S21, A:Q22, A:N23, A:P24, A:V25, A:E26, A:T27, A:S28, A:W29, A:L30, A:S31, A:F32, A:I34, A:L35, A:A36, A:T37, A:R38, A:G39, A:P40, A:C41, A:V42, A:T43, A:S44, A:T45, A:F46, A:L47, A:L49, A:T50, A:V51, A:L54, A:L56	31	0.696
11	A:E537, A:G538, A:T539, A:G540, A:L541	5	0.689
12	A:S57, A:W58, A:S60, A:V61, A:A62, A:V63, A:A64, A:A65, A:H66, A:A67, A:E68, A:H69, A:P70, A:E71, A:D72, A:S73, A:A74, A:T75, A:N76	19	0.682
13	A:A250, A:R251, A:S252, A:L253, A:P317, A:P318, A:R349, A:A352, A:F353, A:L355, A:E356, A:G357, A:L358, A:G359, A:V360, A:Q361, A:V362, A:P363, A:H364, A:R365, A:T366, A:Q367, A:L368, A:A369, A:K370, A:L371, A:I372, A:K374, A:T376, A:S377, A:P378, A:D379, A:P380, A:E381, A:K382, A:R383, A:D392, A:P393, A:F394, A:F395, A:A396, A:S397, A:V398, A:D399, A:R401	45	0.576
14	A:S322, A:L325, A:L326, A:R327, A:K331	5	0.522
15	A:D132, A:E133, A:F134, A:Q135, A:L136, A:T227	6	0.502
16	A:P164, A:S165, A:A166, A:A167	4	0.501

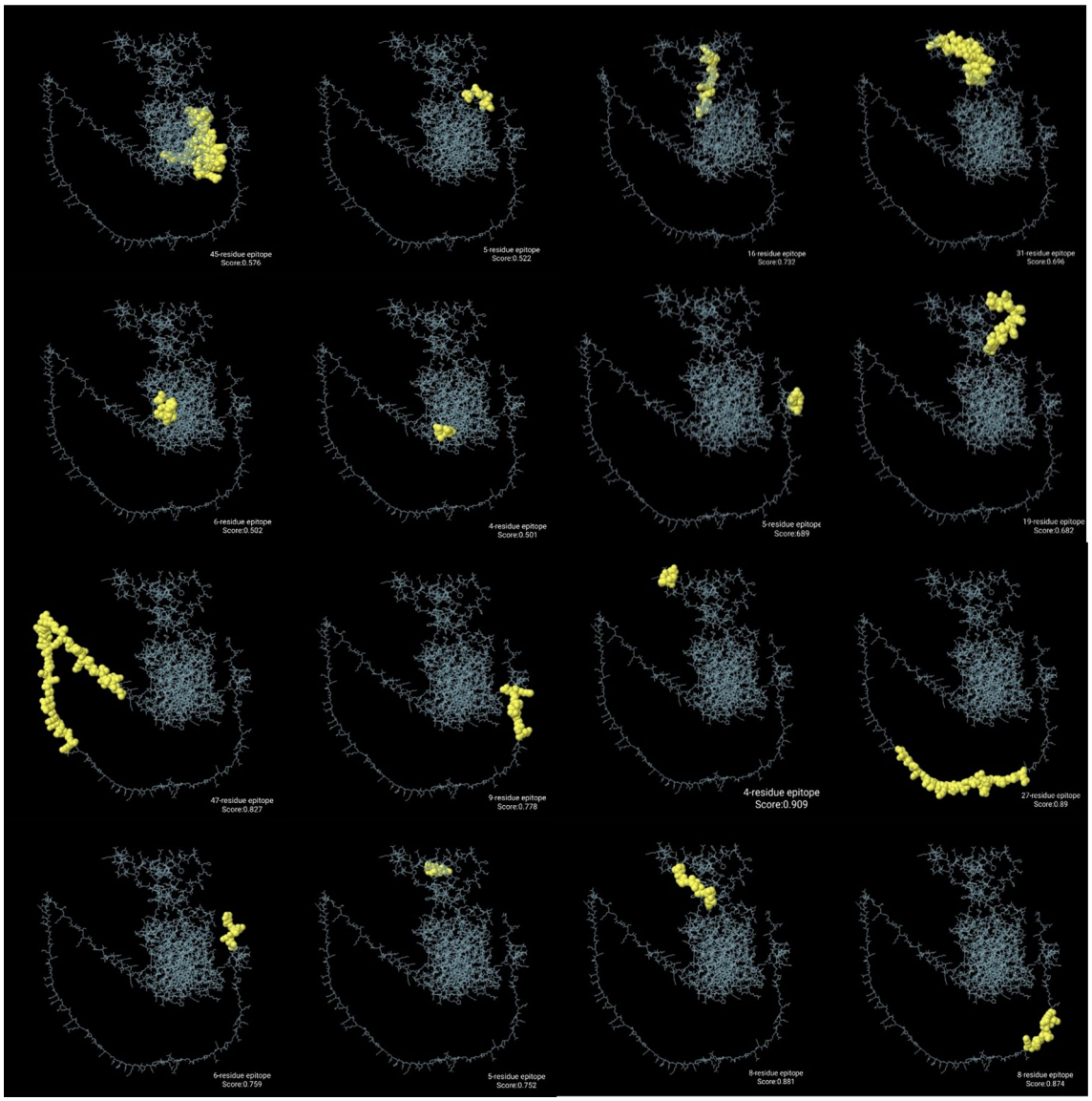

Fig. 11 Predicted conformational B-cell epitopes of *T. gondii* ROP34by ElliPro tool of IEDB Analysis Resource

induction are also indicated. According to the MHC-II outputs and deeper monitoring process concerning immunogenicity, DNFLVSPEGHIVVSD (score: 1.4, immunogenicity: 1.0273) was the most immunogenic epitope amongst other epitopes. Also, according to the MHC-I outputs and deeper monitoring process concerning immunogenicity, EEARSLDFVL (score: 0.51, immunogenicity: 0.03668) was the most immunogenic epitope amongst other epitopes.

3.9 CTL epitope anticipation

According to the results from the CTLpred server, Table 9 contains ten top-ranking 9-mer CTL epitopes of the *T. gondii* ROP34 protein that were anticipated.

Table 7 Percentile rank for ROP34 binding to MHC-I molecules

Allele	Start–end	Peptide Sequence	Percentile Rank	Immunogenicity
H-2Db	165–174	SAALLSFLHL	0.4	−0.05062
	346–355	VAFRHLAFML	0.51	0.14381
	345–354	GVAFRHLAFM	0.65	0.30338
	38–47	RGPCVTSTFL	0.85	−0.03442
	440–449	KAADNAEVPA	1.4	0.18943
H-2-Kb	346–355	VAFRHLAFML	0.07	0.14381
	345–354	GVAFRHLAFM	0.25	0.30338
	44–53	STFLFLTVAF	0.29	0.22428
	165–174	SAALLSFLHL	0.48	−0.05062
	389–398	VMEDPFFASV	0.6	0.20458
H-2-Kk	25–34	VETSWLSFRI	0.1	0.02434
	260–269	AEMAMAVCQL	0.24	−0.22485
	176–185	EEDVPYGVVI	0.25	0.1252
	195–204	FYESVAEPYI	0.36	0.02706
	248–257	EEARSLDFVL	0.51	0.03668
H-2-Dd	38–47	RGPCVTSTFL	0.02	−0.03442
	37–46	TRGPCVTSTF	0.03	−0.09286
	344–353	LGVAFRHLAF	0.29	0.26112
	225–234	RSTSKRVLYL	0.41	−0.28613
	199–208	VAEPYIHRMF	0.44	0.11887
H-2-Kd	195–204	FYESVAEPYI	0.12	0.02706
	307–316	SFLIGTSGYM	0.72	0.07183
	283–292	NFLVSPEGHI	0.78	0.00779
	215–224	PYVVPVLAAL	0.91	0.12978
	149–158	QFFSAGHSKV	0.92	−0.29254
H-2-Ld	163–172	RPSAALLSFL	0.04	−0.06869
	362–371	VPHRTQLAKL	0.14	−0.11584
	23–32	NPVETSWLSF	0.16	0.09334
	316–325	MPPETRSSYL	0.29	−0.11216
	38–47	RGPCVTSTFL	0.31	−0.03442

Low percentile rank = good binders; IC_{50} values = percentile rank

3.10 Immune simulation profile

Based on the C-ImmSim server output, good humoral responses were elicited upon ROP34 protein administration as a vaccine candidate, particularly after the third injection. In this sense, upon antigenic exposure, adequate titers of IgM (~ 300,000), IgG_1 (~ 300,000), and a combination of both [IgG + IgM] (~ 620,000) were predicted (Fig. 12A). Moreover, a high level of the Th-associated cytokine IFN-γ (~ 2,000,000 ng/ml) was provoked by the ROP34 protein of *Toxoplasma* (Fig. 12L). After ROP34 was administered as a vaccine candidate, the Th-cells started to duplicate (approximately five days post exposure), after which active T-CD_4^+ cells were present for approximately 350 days (Fig. 12E, F). A similar trend was detected for T-CD_8^+ cells (T-cytotoxic), which exhibited increasing activity for several weeks post exposure (Fig. 12G, H). The total count of natural killer (NK) cells increased for approximately ten days after antigen exposure, leading to the secretion of IFN-γ and the killing of tachyzoite-infected cells (Fig. 12K, L). More details are illustrated in Fig. 12A–L.

Table 8 Percentile rank for ROP34 binding to MHC-II molecules, antigenicity, IFN-γ and IL-4 induction

Allele	HTL epitope	Percentile rank	Antigenicity	IFN-γ inducing		IL-4 inducing	
				Result	Score	Result	SVM score
H2-IAd	EAREKADAAAKAADN	0.64	0.8170	POSITIVE	1	Non-inducer	−0.31
H2-IAd	AADNAEVPAAKSPAG	0.74	0.6591	POSITIVE	0.30594194	Non-inducer	0.19
H2-IAd	KAADNAEVPAAKSPA	0.83	0.5813	POSITIVE	0.26664146	Non-inducer	0.17
H2-IAd	LEAREKADAAAKAAD	0.85	0.7494	POSITIVE	1	Non-inducer	−0.22
H2-IAd	REKADAAAKAADNAE	0.89	0.7739	POSITIVE	1	Non-inducer	−0.50
H2-IAb	GTSGYMPPETRSSYL	0.35	0.7668	NEGATIVE	−0.84793058	Non-inducer	0.17
H2-IAb	TSGYMPPETRSSYLL	0.5	0.6158	NEGATIVE	−0.5622651	Non-inducer	0.16
H2-IAb	LIGTSGYMPPETRSS	1.1	0.7846	NEGATIVE	−0.76708805	Non-inducer	0.13
H2-IAb	YESVAEPYIHRMFDD	1.2	0.0919	NEGATIVE	−0.70521557	inducer	0.24
H2-IAb	DNFLVSPEGHIVVSD	1.4	1.0273	POSITIVE	1	Non-inducer	−0.30
H2-IEd	RSSYLLRKGYKRSRY	0.24	0.7609	POSITIVE	1	Non-inducer	0.07
H2-IEd	TRSSYLLRKGYKRSR	0.25	0.6825	NEGATIVE	1	Non-inducer	0.06
H2-IEd	SVDFRLVRQRAGKHP	0.3	−0.2004	POSITIVE	1	Non-inducer	0.10
H2-IEd	ASVDFRLVRQRAGKH	0.56	−0.0625	POSITIVE	0.42488037	Non-inducer	0.10
H2-IEd	ETRSSYLLRKGYKRS	0.62	0.4328	POSITIVE	0.17914539	inducer	0.28

Table 9 CTL epitopes predicted with CTLpred server

Peptide rank	Start position	Sequence	Score(ANN/SVM)	Immunogenicity
1	432	REKADAAAK	0.69	0.08368
2	515	QKPSGEENR	1.00	0.0379
3	486	RGRGAQTHE	0.99	0.03162
4	493	HEGNHDRTD	0.99	0.12323
5	447	VPAAKSPAG	0.98	−0.30016
6	450	AKSPAGKTG	0.98	−0.15418
7	478	ERAEEEKGR	0.96	0.143
8	498	DRTDDAGRE	0.96	0.15219
9	446	EVPAAKSPA	0.93	−0.27523
10	480	AEEEKGRGR	0.93	0.01863

4 Discussion

Toxoplasmosis presents a worldwide zoonotic danger with notable public health consequences, affecting pregnant women as well as individuals with weakened immune systems who are at a high risk of infection [6, 9, 55–58]. The host's immune condition enables tachyzoite penetration into different nucleated cells. In those with a healthy immune system, the parasites persist in tissue cysts as bradyzoite stages, potentially leading to opportunistic infections if immunity weakens [59]. Hence, it is essential to devise immunoprophylactic approaches to prevent both immediate and prolonged infections [60]. Vaccination stands out as a prominent prevention strategy, known for improving global living standards [61]. Consequently, vaccination is considered the most logical and effective approach to combat toxoplasmosis. The initial step towards successful vaccine production involves identifying the parasite's potential highly immunoprotective antigens [62]. An essential aspect of creating an effective protein-associated vaccine is employing bioinformatics techniques to assess the antigen's attributes. Bioinformatics is vital in the realm of vaccine development as it forecasts protein structures, functions, and additional biological traits [63]. The core objective of bioinformatics is to advance our comprehension of biological mechanisms and enhance healthcare by pioneering innovative vaccine designs [64]. Rhoptry is a distinctive club-shaped organelle found in *T. gondii*. Only these apical secretory organelles are common to all parasitic apicomplexans [65]. Rhoptry proteins are essential for the survival of parasites within host cells and play a role in the various stages of their invasion [20, 65, 66]. Because of this, ROPs have gained attention lately and are being

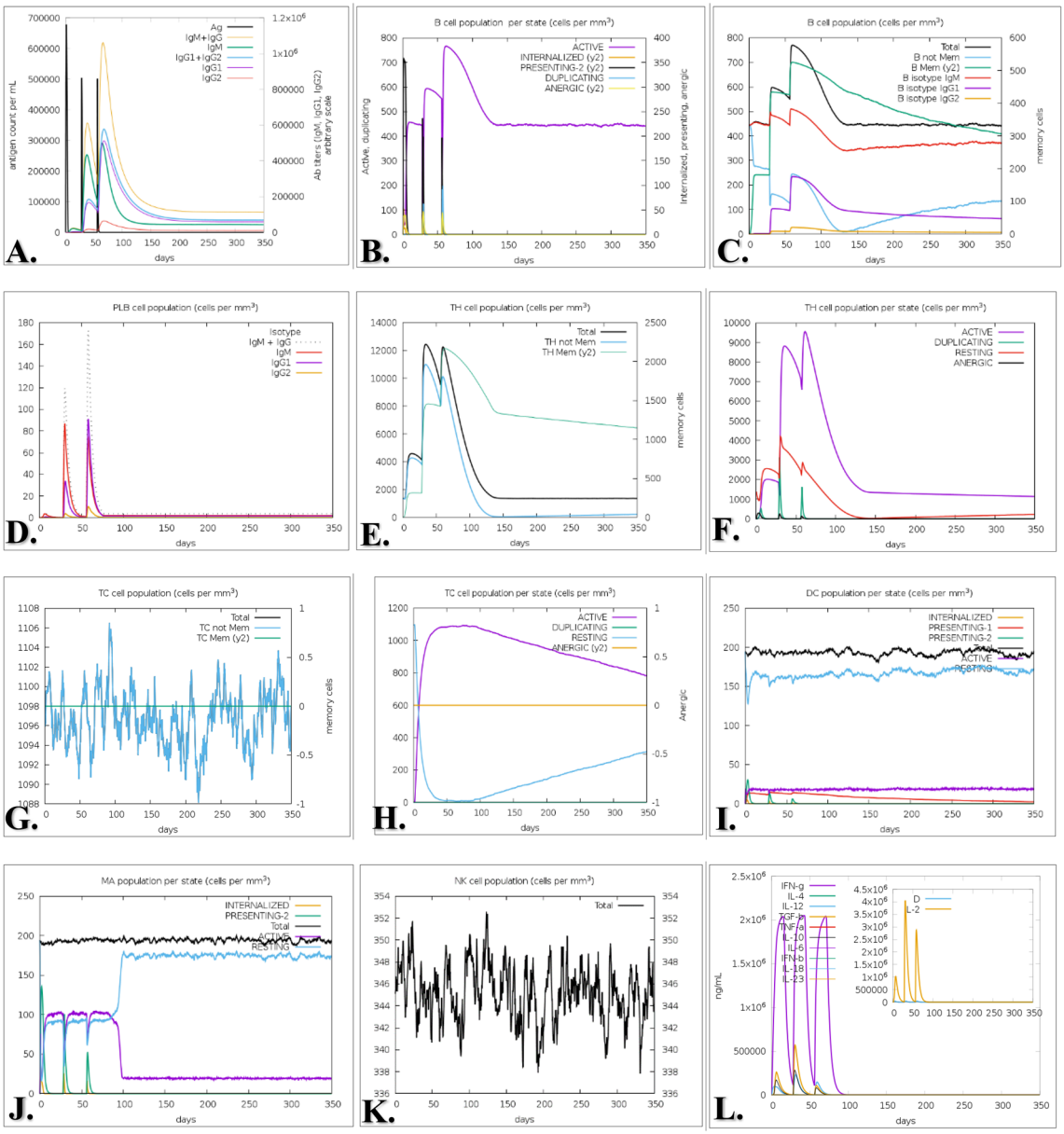

Fig. 12 silico immune simulation. **A** immunoglobulin production in response to ROP34; **B**, **C** B lymphocytes population; **D** plasma B lymphocytes count sub-divided per isotype (IgM, IgG1 and IgG2); **E**, **F** TH cell (CD4 +) population; **G**, **H** TC cell (CD8 +) population; **I** dendritic cells per state; **J** macrophage population per state; **K** NK cell population; and **L** level of cytokines production (ng/ml) by ROP34

considered as potential toxoplasmosis vaccine candidates. According to earlier articles, several ROPs showed positive and promising results [67, 68]. However, the structure and epitopes of ROP34 remain not well-defined.

According to ProtParam results, ROP34 is an appropriate immunogenic compound, with a MW of 61.60149 KDa (antigens with a MW of greater than 5–10 KDa are regarded as strong immunogens) [8]. However, the instability index of ROP34 was calculated to be 49.66. The research also illustrated the enhanced thermotolerance of ROP34, boasting an AI score of 73.98, suggesting that the protein exhibits increased stability over different temperatures. The GRAVY score of − 0.554 indicates that ROP34 is hydrophilic, making it better suited for water-based environments. The isoelectric point (pI) of 6.29 suggests that the protein could be effectively purified using isoelectric focusing and ion-exchange chromatography. These fundamental biochemical characteristics are beneficial for forthcoming extraction and purification procedures in experimental studies. ANTIGENpro and VaxiJen analyses confirmed the protein's immunogenicity, while AlgPred and SOLpro servers indicated that the protein is non-allergenic with a predicted insolubility of 0.598154. Despite its insolubility, the protein can be re-dissolved by adjusting detergent, ionic strength, pH, or dilution during purification

assays to enhance protein yield [69]. The extinction coefficient of ROP34, which gauges the substance's light absorption efficiency at a specific wavelength, was established at 29,005 M^{-1} cm^{-1} in water at 280 nm. The secretory apparatus and the existence of signal peptides impact the output of recombinant protein manufacturing. The latter, also known as leader sequences, are typically short peptides located at the N-terminus of newly produced proteins, containing codes associated with the protein secretion pathway and target site. As per the findings, ROP34 features a conventional SPI/Sec signal peptide with a probability of 0.9878. The SPI/Sec signal peptides are conventional secretory signals that are cleaved by Signal Peptidase I and conveyed by the Sec translocon [70]. Proteins synthesized in their crude form commonly undergo diverse enzymatic alterations like phosphorylation and acylation, recognized as PTMs [71]. The existence of PTMs in eukaryotic cells, encompassing parasites, like *T. gondii*, is vital in determining the suitable expression system for creating recombinant proteins [72]. In this research, we utilized GPS-PAIL and NetPhos 3.1 servers to forecast PTM locations within the ROP34 protein sequence. A total of 44 PTM sites were identified, consisting of 40 phosphorylation sites and 4 acylation sites, which notably influence the protein's biological role. Furthermore, we verified N- and O-linked glycosylation sites, which are crucial PTMs [18]. Considering these results, when aiming to produce the *T. gondii* ROP34 protein together with other desired proteins in a recombinant manner, it is essential to take into account the presence of phosphorylation, N-linked glycosylation, and acetylation areas. Given this situation, it is advisable to prioritize eukaryotic expression systems like mammals, yeast, and insects over bacterial systems. No potential transmembrane domain aids in antigen presentation, eliciting both cellular and humoral immune responses, ensuring a swift reaction [8]. Generally, the organization of hydrogen bonds between amino carboxyl oxygen and hydrogen atoms in a polypeptide chain dictates the secondary structure, predominantly comprising β-structures and α-helices [73]. Furthermore, the distinct interactions and bonds within a protein molecule govern its tertiary structure. The existence of beta-turn and alpha-helix within the protein configuration, coupled with significant hydrogen-bond energy, assists in upholding protein conformation and facilitates effective interaction with antibodies [16]. As per the GOR IV and PSIPRED servers, the secondary structure of the protein consists of 36.17% alpha helix, 52.80% random coil, and 11.03% extended strand. Subsequently, the most suitable model from 50 templates of tertiary structures was chosen for additional examination. The GalaxyRefine server reconstructed and optimized side-chains within the selected 3D model, notably enhancing the total quality by molecular dynamics simulation [74]. The refined model was chosen based on several quality factors, including RMSD (0.549), GDT-HA (0.9222), MolProbity (1.498), Poor rotamers (0.2), Clash score (7.1), and Rama favored (97.5). GDT-HA assesses the protein model's general quality, whereas RMSD gauges the variance in bond lengths and angles between the initial and enhanced models. A reduced RMSD suggests that the refined model closely resembles the initial structure. As per Chen et al., "a structure with a MolProbity score lower than its crystallographic resolution is considered superior in quality compared to an average structure at that resolution" [75, 76]. The clash score indicates steric clashes within the refined model, influenced by the resolution of the protein structure. The limited ability of specific residues to rotate within their side chains leads to suboptimal rotamers. The outcomes from ProSA-web additionally emphasized improvements in the general quality of the refined model in contrast to the original model. The innate immune response pathways to deal with *T. gondii* establish the foundation for the subsequent triggering of adaptive immunity, which includes both humoral and cellular immune reactions [77]. One benefit of in silico vaccination approaches is their ability to directly stimulate strong immunity, efficiently controlling the parasite. This procedure entails pinpointing epitopes for B-cells, CTLs, and MHC-binding regions of a specific protein using various online resources [19, 78]. The ABCpred server, employing an ANN-oriented fixed-length pattern, forecasted linear B-cell epitopes with an accuracy of 65.93%. Bcepred anticipated continuous B-cell epitopes by considering factors like polarity, hydrophilicity, flexibility, accessibility, turns, and antigenic propensity, achieving accuracies ranging from 58.7% [45, 46]. The SVMTriP Database estimated the B-cell epitopes depending on the Tri-peptide correlation and Propensity values [48]. Another important step in the bioinformatic analysis of a vaccine candidate is the determination of conformational epitopes to improve antigen–antibody interaction. Therefore, the ElliPro tool has been well adopted. Protozoa induce humoral and cellular immune responses in the host. Immunoglobulins, especially IgG, inhibit the binding of parasite adhesions and enhance cellular phagocytosis through the process of opsonization. Note that the most protective immune mechanism against toxoplasmosis is through CD_4^+ and CD_8^+ T cells and IFN-γ cytokines, which together limit parasite invasion and reproduction [60, 79]. The IEDB online tool revealed epitopes with increased binding affinity to MHC-II and MHC-I. As mentioned earlier, lower IC_{50} scores (or percentile ranks) indicate a higher level of affinity. Furthermore, the CTLpred server identified a total of 10 CTL-specific epitopes, crucial for the design of a toxoplasmosis vaccine. The combined and consensus prediction techniques of CTLpred exhibit higher accuracy compared to the ANN and SVM alternatives[52]. We have also shown that the ROP34 protein can elicit adequate humoral and cell-mediated immune reactions, considering the antibody titers and cytokine levels induced by the administration of the ROP34 protein, as evidenced by the C-ImmSim web server. Although our study was

only done in silico, the results of previous studies on this gene, similar to our study, show that ROPs can increase survival in mice. DNA vaccine encoding MIC3 and ROP18 of *T. gondii* immunized in mice demonstrated that mice immunized with pROP18-MIC3 elicited stronger humoral and Th1 cellular immune responses, as well as longer survival times against toxoplasmosis [80]. Another study which was done on GRA7 and ROP1 of *T. gondii,* the results showed increased IgG2a titers, IFN-γ and TNF-α production, survival duration, and cyst reduction rate [81].

Numerous publications discuss ROP-based vaccines that utilized a combination of bioinformatics online servers and various softwares to predict potential B and T cell epitopes, resulting in an excellent vaccine candidate to prevent toxoplasmosis. Nevertheless, there is insufficient evidence to support the protective effectiveness of certain of them in animal models [82–87]. It is strongly advised that more research be done in the future using both in silico and in vivo methods to assess the potency of protein as a likely vaccine candidate, since the immunogenicity of the predicted sequences by various bioinformatics approaches should be confirmed in an appropriate mouse model.

5 Conclusion

Computer-based technologies have afforded humankind an opportunity to more effectively address health issues encountered, including enhanced strategies for preventing infectious diseases. Toxoplasmosis represents a significant global concern, especially for pregnant individuals and those with weakened immune systems. Innovative bioinformatics tools have facilitated a deeper comprehension of the immunoprotective domains within antigenic molecules through immunosense methodologies, contributing to improved vaccine design against diverse infectious pathogens. In this context, we present insightful bioinformatics insights regarding the *Toxoplasma* ROP34 protein, demonstrating its potential as a future vaccine choice in in silico multi-epitope-associated vaccinology studies. Nevertheless, empirical evaluation of the effectiveness and strength of these candidate proteins, in conjunction with many antigenic epitopes, substances, and/or formulations is recommended.

Author contributions A. Dalir Ghaffari, F. Mohammadhasani, and M. Asadi conceived the study and designed the study protocol; A. Dalir Ghaffari wasthe supervisor of this research; A. Dalir Ghaffari F. Mohammadhasani, and M. Asadi performed the whole bioinformatics analyses; all authors drafted the manuscript and approved the final version of the manuscript.

Funding Not applicable.

Data availability Data availability statement: The datasets used and/or analysed during the current study available from the corresponding author on reasonable request.

Declarations

Competing interests The authors declare no competing interests.

References

1. Rostami A, Riahi SM, Fakhri Y, Saber V, Hanifehpour H, Valizadeh S, et al. The global seroprevalence of *Toxoplasma gondii* among wild boars: a systematic review and meta-analysis. Vet Parasitol. 2017;244:12–20.
2. Dubey JP. The history of *Toxoplasma gondii*—the first 100 years. J Eukaryot Microbiol. 2008;55:467–75.
3. Khademvatan S, Saki J, Yousefi E, Abdizadeh R. Detection and genotyping of *Toxoplasma gondii* strains isolated from birds in the southwest of Iran. Br Poult Sci. 2013;54:76–80.

4. Meng M, He S, Zhao G, Bai Y, Zhou H, Cong H, et al. Evaluation of protective immune responses induced by DNA vaccines encoding *Toxoplasma gondii* surface antigen 1 (SAG1) and 14-3-3 protein in BALB/c mice. Parasit Vectors. 2012;5:1–10.
5. Tenter AM, Heckeroth AR, Weiss LM. *Toxoplasma gondii*: from animals to humans. Int J Parasitol. 2000;30:1217–58.
6. Belluco S, Mancin M, Conficoni D, Simonato G, Pietrobelli M, Ricci A. Investigating the determinants of *Toxoplasma gondii* prevalence in meat: a systematic review and meta-regression. PLoS ONE. 2016;11: e0153856.
7. Daryani A, Sarvi S, Aarabi M, Mizani A, Ahmadpour E, Shokri A, et al. Seroprevalence of *Toxoplasma gondii* in the Iranian general population: a systematic review and meta-analysis. Acta Trop. 2014;137:185–94.
8. Ghaffari AD, Dalimi A, Ghaffarifar F, Pirestani M. Structural predication and antigenic analysis of ROP16 protein utilizing immunoinformatics methods in order to identification of a vaccine against *Toxoplasma gondii*: an in silico approach. Microb Pathog. 2020;142: 104079.
9. Wang Z-D, Liu H-H, Ma Z-X, Ma H-Y, Li Z-Y, Yang Z-B, et al. *Toxoplasma gondii* infection in immunocompromised patients: a systematic review and meta-analysis. Front Microbiol. 2017;8: 238621.
10. Kravetz JD, Federman DG. Toxoplasmosis in pregnancy. Am J Med. 2005;118:212–6.
11. Luft BJ, Remington JS. Toxoplasmic encephalitis in AIDS. Clin Infect Dis. 1992;15:211–22.
12. Dziadek B, Gatkowska J, Brzostek A, Dziadek J, Dzitko K, Grzybowski M, et al. Evaluation of three recombinant multi-antigenic vaccines composed of surface and secretory antigens of *Toxoplasma gondii* in murine models of experimental toxoplasmosis. Vaccine. 2011;29:821–30.
13. Díaz E, Köhidai L, Ríos A, Vanegas O, Silva A, Szabó R, et al. Leishmania braziliensis: cytotoxic, cytostatic and chemotactic effects of poly-lysine–methotrexate-conjugates. Exp Parasitol. 2013;135:134–41.
14. Ram H, Rao J, Tewari A, Banerjee P, Sharma A. Molecular cloning, sequencing, and biological characterization of GRA4 gene of *Toxoplasma gondii*. Parasitol Res. 2013;112:2487–94.
15. Romano P, Giugno R, Pulvirenti A. Tools and collaborative environments for bioinformatics research. Brief Bioinform. 2011;12:549–61.
16. Shaddel M, Ebrahimi M, Tabandeh MR. Bioinformatics analysis of single and multi-hybrid epitopes of GRA-1, GRA-4, GRA-6 and GRA-7 proteins to improve DNA vaccine design against *Toxoplasma gondii*. J Parasit Dis. 2018;42:269–76.
17. Wang Y, Wang G, Zhang D, Yin H, Wang M. Identification of novel B cell epitopes within *Toxoplasma gondii* GRA1. Exp Parasitol. 2013;135:606–10.
18. Can H, Alak SE, Köseoğlu AE, Döşkaya M, Ün C. Do *Toxoplasma gondii* apicoplast proteins have antigenic potential? An in silico study. Comput Biol Chem. 2020;84: 107158.
19. Foroutan M, Ghaffarifar F, Sharifi Z, Dalimi A. Vaccination with a novel multi-epitope ROP8 DNA vaccine against acute *Toxoplasma gondii* infection induces strong B and T cell responses in mice. Comp Immunol Microbiol Infect Dis. 2020;69: 101413.
20. Dlugonska H. Toxoplasma rhoptries: unique secretory organelles and source of promising vaccine proteins for immunoprevention of toxoplasmosis. J Biomed Biotechnol. 2008. https://doi.org/10.1155/2008/632424.
21. Nabi H, Rashid I, Ahmad N, Durrani A, Akbar H, Islam S, et al. Induction of specific humoral immune response in mice immunized with ROP18 nanospheres from *Toxoplasma gondii*. Parasitol Res. 2017;116:359–70.
22. Wang H-L, Wang Y-J, Pei Y-J, Bai J-Z, Yin L-T, Guo R, et al. DNA vaccination with a gene encoding *Toxoplasma gondii* Rhoptry Protein 17 induces partial protective immunity against lethal challenge in mice. Parasite. 2016. https://doi.org/10.1051/parasite/2016004.
23. Wang L, Lu G, Zhou A, Han Y, Guo J, Zhou H, et al. Evaluation of immune responses induced by rhoptry protein 5 and rhoptry protein 7 DNA vaccines against *Toxoplasma gondii*. Parasite Immunol. 2016;38:209–17.
24. Zhou J, Wang L, Lu G, Zhou A, Zhu M, Li Q, et al. Epitope analysis and protection by a ROP19 DNA vaccine against *Toxoplasma gondii*. Parasite. 2016. https://doi.org/10.1051/parasite/2016017.
25. Gasteiger E, Hoogland C, Gattiker A, Duvaud S, Wilkins MR, Appel RD, Bairoch A. Protein identification and analysis tools on the ExPASy server. In: Walker JM, editor. The proteomics protocols handbook. Totowa: Humana Press; 2005. p. 571–607. https://doi.org/10.1385/1-59259-890-0:571.
26. Magnan CN, Zeller M, Kayala MA, Vigil A, Randall A, Felgner PL, et al. High-throughput prediction of protein antigenicity using protein microarray data. Bioinformatics. 2010;26:2936–43.
27. Doytchinova IA, Flower DR. VaxiJen: a server for prediction of protective antigens, tumour antigens and subunit vaccines. BMC Bioinf. 2007;8:1–7.
28. Saha S, Raghava GPS. AlgPred: prediction of allergenic proteins and mapping of IgE epitopes. Nucleic Acids Res. 2006;34:W202–9.
29. Magnan CN, Randall A, Baldi P. SOLpro: accurate sequence-based prediction of protein solubility. Bioinformatics. 2009;25:2200–7.
30. Petersen TN, Brunak S, Von Heijne G, Nielsen H. SignalP 4.0: discriminating signal peptides from transmembrane regions. Nat Methods. 2011;8:785–6.
31. Blom N, Gammeltoft S, Brunak S. Sequence and structure-based prediction of eukaryotic protein phosphorylation sites. J Mol Biol. 1999;294:1351–62.
32. Deng W, Wang C, Zhang Y, Xu Y, Zhang S, Liu Z, et al. GPS-PAIL: prediction of lysine acetyltransferase-specific modification sites from protein sequences. Sci Rep. 2016;6:39787.
33. Blom N, Sicheritz-Pontén T, Gupta R, Gammeltoft S, Brunak S. Prediction of post-translational glycosylation and phosphorylation of proteins from the amino acid sequence. Proteomics. 2004;4:1633–49.
34. Steentoft C, Vakhrushev SY, Joshi HJ, Kong Y, Vester-Christensen MB, Schjoldager KTB, et al. Precision mapping of the human O-GalNAc glycoproteome through SimpleCell technology. EMBO J. 2013;32:1478–88.
35. Zhou J, Wang L, Zhou A, Lu G, Li Q, Wang Z, et al. Bioinformatics analysis and expression of a novel protein ROP48 in *Toxoplasma gondii*. Acta Parasitol. 2016;61:319–28.
36. Garnier J, Gibrat J-F, Robson B. [32] GOR method for predicting protein secondary structure from amino acid sequence. In: Computer methods for macromolecular sequence analysis. Elsevier; 1996. p. 540–53. https://doi.org/10.1016/S0076-6879(96)66034-0.
37. Buchan DW, Jones DT. The PSIPRED protein analysis workbench: 20 years on. Nucleic Acids Res. 2019;47:W402–7.
38. Fahimi H, Sadeghizadeh M, Mohammadipour M. In silico analysis of an envelope domain III-based multivalent fusion protein as a potential dengue vaccine candidate. Clin Exp Vacc Res. 2016;5:41.

39. Guex N, Peitsch MC, Schwede T. Automated comparative protein structure modeling with SWISS-MODEL and Swiss-PdbViewer: a historical perspective. Electrophoresis. 2009;30:S162–73.
40. Ko J, Park H, Heo L, Seok C. GalaxyWEB server for protein structure prediction and refinement. Nucleic Acids Res. 2012;40:W294–7.
41. Nugent T, Cozzetto D, Jones DT. "Evaluation of predictions in the CASP10 model refinement category. Proteins Struct Funct Bioinf. 2014;82:98–111.
42. Bertoni M, Kiefer F, Biasini M, Bordoli L, Schwede T. Modeling protein quaternary structure of homo-and hetero-oligomers beyond binary interactions by homology. Sci Rep. 2017;7:10480.
43. Narula A, Pandey RK, Khatoon N, Mishra A, Prajapati VK. Excavating chikungunya genome to design B and T cell multi-epitope subunit vaccine using comprehensive immunoinformatics approach to control chikungunya infection. Infect Genet Evol. 2018;61:4–15.
44. Saha S, Raghava GPS. "Prediction of continuous B-cell epitopes in an antigen using recurrent neural network. Proteins Struct Funct Bioinf. 2006;65:40–8.
45. Kazi A, Chuah C, Majeed ABA, Leow CH, Lim BH, Leow CY. Current progress of immunoinformatics approach harnessed for cellular- and antibody-dependent vaccine design. Pathog Glob Health. 2018;112:123–31.
46. Saha S, Raghava GPS BcePred: prediction of continuous B-cell epitopes in antigenic sequences using physico-chemical properties. In: International conference on artificial immune systems 2004; 197–204.
47. EL-Manzalawy Y, Dobbs D, Honavar V. Predicting linear B-cell epitopes using string kernels. J Mol Recog Interdiscip J. 2008;21:243–55.
48. Yao B, Zhang L, Liang S, Zhang C. SVMTriP: a method to predict antigenic epitopes using support vector machine to integrate tri-peptide similarity and propensity. PLoS ONE. 2012;7(9):e45152. https://doi.org/10.1371/journal.pone.0045152.
49. Ponomarenko J, Bui H-H, Li W, Fusseder N, Bourne PE, Sette A, et al. ElliPro: a new structure-based tool for the prediction of antibody epitopes. BMC Bioinf. 2008;9:1–8.
50. Dimitrov I, Naneva L, Doytchinova I, Bangov I. AllergenFP: allergenicity prediction by descriptor fingerprints. Bioinformatics. 2014;30:846–51.
51. Calis JJ, Maybeno M, Greenbaum JA, Weiskopf D, De Silva AD, Sette A, et al. Properties of MHC class I presented peptides that enhance immunogenicity. PLoS Comput Biol. 2013;9: e1003266.
52. Bhasin M, Raghava GP. Prediction of CTL epitopes using QM, SVM and ANN techniques. Vaccine. 2004;22:3195–204.
53 Rapin N, Lund O, Bernaschi M, Castiglione F. Computational immunology meets bioinformatics: the use of prediction tools for molecular binding in the simulation of the immune system. PLoS ONE. 2010;5:e9862.
54 Castiglione F, Mantile F, De Berardinis P, Prisco A. How the interval between prime and boost injection affects the immune response in a computational model of the immune system. Comput Math Methods Med. 2012. https://doi.org/10.1155/2012/842329.
55. Foroutan-Rad M, Khademvatan S, Majidiani H, Aryamand S, Rahim F, Malehi AS. Seroprevalence of *Toxoplasma gondii* in the Iranian pregnant women: a systematic review and meta-analysis. Acta Trop. 2016;158:160–9.
56. Foroutan-Rad M, Majidiani H, Dalvand S, Daryani A, Kooti W, Saki J, et al. Toxoplasmosis in blood donors: a systematic review and meta-analysis. Transfus Med Rev. 2016;30:116–22.
57. Weiss LM, Dubey JP. Toxoplasmosis: a history of clinical observations. Int J Parasitol. 2009;39:895–901.
58 Sharif M, Sarvi S, Shokri A, HosseiniTeshnizi S, Rahimi M, Mizani A, et al. *Toxoplasma gondii* infection among sheep and goats in Iran: a systematic review and meta-analysis. Parasitol Res. 2015;114:1–16.
59. Ahmadpour E, Daryani A, Sharif M, Sarvi S, Aarabi M, Mizani A, et al. Toxoplasmosis in immunocompromised patients in Iran: a systematic review and meta-analysis. J Infect Dev Ctries. 2014;8:1503–10.
60. Jongert E, Roberts CW, Gargano N, Förster-Waldl E, Petersen E. Vaccines against *Toxoplasma gondii*: challenges and opportunities. Mem Inst Oswaldo Cruz. 2009;104:252–66.
61. Yaqub O, Castle-Clarke S, Sevdalis N, Chataway J. Attitudes to vaccination: a critical review. Soc Sci Med. 2014;112:1–11.
62. Wang Y, Wang G, Cai J, Yin H. Review on the identification and role of *Toxoplasma gondii* antigenic epitopes. Parasitol Res. 2016;115:459–68.
63. Zhang N-Z, Chen J, Wang M, Petersen E, Zhu X-Q. Vaccines against *Toxoplasma gondii*: new developments and perspectives. Expert Rev Vaccines. 2013;12:1287–99.
64. Hiszczyńska-Sawicka E, Olędzka G, Holec-Gąsior L, Li H, Xu JB, Sedcole R, et al. Evaluation of immune responses in sheep induced by DNA immunization with genes encoding GRA1, GRA4, GRA6 and GRA7 antigens of *Toxoplasma gondii*. Vet Parasitol. 2011;177:281–9.
65. Bradley PJ, Sibley LD. Rhoptries: an arsenal of secreted virulence factors. Curr Opin Microbiol. 2007;10:582–7.
66. Dubremetz JF. Rhoptries are major players in *Toxoplasma gondii* invasion and host cell interaction. Cell Microbiol. 2007;9:841–8.
67. Khosroshahi KH, Ghaffarifar F, Sharifi Z, D'Souza S, Dalimi A, Hassan ZM, et al. Comparing the effect of IL-12 genetic adjuvant and alum non-genetic adjuvant on the efficiency of the cocktail DNA vaccine containing plasmids encoding SAG-1 and ROP-2 of *Toxoplasma gondii*. Parasitol Res. 2012;111:403–11.
68. Kur J, Holec-Gąsior L, Hiszczyńska-Sawicka E. Current status of toxoplasmosis vaccine development. Expert Rev Vaccines. 2009;8:791–808.
69. Janson J-C. Protein purification: principles, high resolution methods, and applications. Hoboken: Wiley; 2012.
70. Owji H, Nezafat N, Negahdaripour M, Hajiebrahimi A, Ghasemi Y. A comprehensive review of signal peptides: structure, roles, and applications. Eur J Cell Biol. 2018;97:422–41.
71. Walsh C. Posttranslational modification of proteins: expanding nature's inventory. Greenwood Village: Roberts and Company Publishers; 2006.
72. Hansson M, Nygren PAK, Sta˚hl S. Design and production of recombinant subunit vaccines. Biotechnol Appl Biochem. 2000;32:95–107.
73. Yadav G, Rao R, Raj U, Varadwaj PK. Computational modeling and analysis of prominent T-cell epitopes for assisting in designing vaccine of ZIKA virus. J Appl Pharm Sci. 2017;7:116–22.
74. Heo L, Park H, Seok C. GalaxyRefine: protein structure refinement driven by side-chain repacking. Nucleic Acids Res. 2013;41:W384–8.
75. Chen J, Liu H, Yang J, Chou K-C. Prediction of linear B-cell epitopes using amino acid pair antigenicity scale. Amino Acids. 2007;33:423–8.
76. Chen VB, Arendall WB, Headd JJ, Keedy DA, Immormino RM, Kapral GJ, et al. MolProbity: all-atom structure validation for macromolecular crystallography. Acta Crystallogr D Biol Crystallogr. 2010;66:12–21.
77. Sasai M, Yamamoto M. Innate, adaptive, and cell-autonomous immunity against *Toxoplasma gondi*i infection. Exp Mol Med. 2019;51:1–10.

78. Foroutan M, Ghaffarifar F, Sharifi Z, Dalimi A, Pirestani M. Bioinformatics analysis of ROP8 protein to improve vaccine design against *Toxoplasma gondii*. Infect Genet Evol. 2018;62:193–204.
79. Lang C, Groß U, Lüder CG. Subversion of innate and adaptive immune responses by *Toxoplasma gondii*. Parasitol Res. 2007;100:191–203.
80. Qu D, Han J, Du A. Evaluation of protective effect of multiantigenic DNA vaccine encoding MIC3 and ROP18 antigen segments of *Toxoplasma gondii* in mice. Parasitol Res. 2013;112:2593–9.
81. Quan J-H, Chu J-Q, Ismail HAHA, Zhou W, Jo E-K, Cha G-H, et al. Induction of protective immune responses by a multiantigenic DNA vaccine encoding GRA7 and ROP1 of *Toxoplasma gondii*. Clin Vaccine Immunol. 2012;19:666–74.
82. Cao A, Liu Y, Wang J, Li X, Wang S, Zhao Q, et al. *Toxoplasma gondii*: vaccination with a DNA vaccine encoding T-and B-cell epitopes of SAG1, GRA2, GRA7 and ROP16 elicits protection against acute toxoplasmosis in mice. Vaccine. 2015;33:6757–62.
83. Cong H, Gu QM, Yin HE, Wang JW, Zhao QL, Zhou HY, et al. Multi-epitope DNA vaccine linked to the A2/B subunit of cholera toxin protect mice against *Toxoplasma gondii*. Vaccine. 2008;26:3913–21.
84. Wang T, Yin H, Li Y, Zhao L, Sun X, Cong H. Vaccination with recombinant adenovirus expressing multi-stage antigens of *Toxoplasma gondii* by the mucosal route induces higher systemic cellular and local mucosal immune responses than with other vaccination routes. Parasite. 2017;24:12.
85. Yin H, Zhao L, Wang T, Zhou H, He S, Cong H. A *Toxoplasma gondii* vaccine encoding multistage antigens in conjunction with ubiquitin confers protective immunity to BALB/c mice against parasite infection. Parasit Vectors. 2015;8:1–11.
86. Zhou J, Lu G, Wang L, Zhou AH, Han YL, Guo JJ, et al. Structuraland antigenic analysis of a new Rhoptry Pseudokinase Gene (ROP54) in *Toxoplasma gondii*. Acta Parasitol. 2017;62:513–9.
87. Zhou J, Wang W, Song P, Wang L, Han Y, Guo J, et al. Structural predication and antigenic analysis of *Toxoplasma gondii* ROP20. Acta Parasitol. 2018;63:244–51.